Using GRENOUILLE to characterize asymmetric femtosecond pulses undergoing self- and cross-phase modulation in a polarization-maintaining optical fiber

Bhaskar Khubchandani and A. Christian Silva
Department of Physics and IREAP, University of Maryland, College Park, Maryland, 20742
bhaskark@physics.umd.edu, silvaac@glue.umd.edu

Parvez N. Guzdar
IREAP, University of Maryland, College Park, Maryland 20742
guzdar@glue.umd.edu

Rajarshi Roy
Department of Physics, IREAP and IPST, University of Maryland, College Park, Maryland 20742
rroy@glue.umd.edu

Abstract: Self- and Cross-phase modulation of asymmetric femtosecond pulses ($\sim$ 810 nm) propagating through a birefringent single-mode optical fiber ($\sim$ 6.9 cm) is studied both experimentally (using GRENOUILLE) and numerically (by solving a set of coupled nonlinear Schrödinger equations or CNLSEs). An optical spectrogram representation is derived from the electric field of the pulses and is linearly juxtaposed with the corresponding optical spectrum and optical time-trace. The simulations are shown to be in good qualitative agreement with the experiments. Measured input pulse asymmetry, when incorporated into the simulations, is found to be the dominant cause of output spectral asymmetry. The results indicate that it is possible to modulate short pulses both temporally and spectrally by passage through polarization maintaining optical fibers with specified orientation and length.

© 2003 Optical Society of America

OCIS codes: (060.0060) Fiber optics and optical communications; (060.2330) Optical fiber communication; (320.7100) ultrafast measurements; (060.2420) Fibers, polarization maintaining; (190.4380) Nonlinear optics, four wave mixing

References and links

1. R. Trebino, *Frequency-Resolved Optical Gating: The Measurement of Ultrashort Laser Pulses* (Kluwer Academic, 2002).
2. G.P. Agrawal, *Nonlinear Fiber Optics* (Academic, San Diego, 2001).
3. J.M. Dudley, X. Gu, L. Xu, M. Kimmel, E. Zeek, P. O'Shea, R. Trebino, S. Coen, R.S. Windeler, "Cross-correlation frequency resolved optical gating analysis of broadband continuum generation in photonic crystal fiber: simulations and experiments," Opt. Express **10**, 1215 (2002), http://www.opticsexpress.org/abstract.cfm?URI=OPEX-10-21-1215.
4. Q. D. Liu, J. T. Chen, Q. Z. Wang, P. P. Ho, and R. R. Alfano, "Single pulse degenerate-cross-phase modulation in a single-mode optical fiber," Opt. Lett. 20, 542-544 (1995).

#3084 - $15.00 US Received Septebmer 25, 2003; Revised October 31, 2003

5. T. Sylvestre, H. Maillotte, E. Lantz, and D. Gindre "Combined spectral effects of pulse walk-off and degenerate cross-phase modulation in birefringent fibers," Journal of Nonlinear Optical Physics and Materials 6, 313-320 (1997).
6. Q. D. Liu, L. Shi, P. P. Ho, R. R. Alfano, R.-J. Essiambre, and G.P. Agrawal, "Degenerate cross-phase modulation of femtosecond laser pulses in a birefringent single-mode fiber," IEEE Photon. Tech. Lett. 9, 1107-1109 (1997).
7. F.G. Omenetto, B.P. Luce, D. Yarotski and A.J. Taylor, "Observation of chirped soliton dynamics at l= 1.55 mm in a single-mode optical fiber with frequency-resolved optical gating," Opt. Lett. **24**, 1392 (1999).
8. F.G. Omenetto, Y. Chung, D. Yarotski, T. Shaefer, I. Gabitov and A.J. Taylor, "Phase analysis of nonlinear femtosecond pulse propagation and self-frequency shift in optical fibers," Opt. Commun. **208**, 191 (2002).
9. F.G. Omenetto, J.W. Nicholson, B.P. Luce, D. Yarotski, A.J. Taylor, "Shaping, propagation and characterization of ultrafast pulses in optical fibers," Appl. Phys. B **70**[Suppl.], S143 (2000).
10. N. Nishizawa and T. Goto, "Experimental analysis of ultrashort pulse propagation in optical fibers around zero-dispersion region using cross-correlation frequency resolved optical gating," Opt. Express **8**, 328 (2001), http://www.opticsexpress.org/abstract.cfm?URI=OPEX-8-6-328.
11. N. Nishizawa and T. Goto, "Trapped pulse generation by femtosecond soliton pulse in birefringent optical fibers," Opt. Express **10**, 256 (2002), http://www.opticsexpress.org/abstract.cfm?URI=OPEX-10-5-256.
12. N. Nishizawa and T. Goto, "Characteristics of pulse trapping by use of ultrashort soliton pulses in optical fibers across the zero-dispersion wavelength," Opt. Express **10**, 1151 (2002), http://www.opticsexpress.org/abstract.cfm?URI=OPEX-10-21-1151.
13. N. Nishizawa and T. Goto, "Ultrafast all optical switching by use of pulse trapping across zero-dispersion wavelength," Opt. Express **11**, 359 (2003), http://www.opticsexpress.org/abstract.cfm?URI=OPEX-11-4-359.
14. K. Ogawa, M.D. Pelusi, "Characterization of ultrashort optical pulses in a dispersion-managed fiber link using two-photon absorption frequency-resolved optical gating," Opt. Commun. **198**, 83-87 (2001).
15. R.A. Altes, "Detection, estimation, and classification with spectrograms," J. Acoust. Soc. Am. 674, 1232 (1980).
16. P. O'Shea, M. Kimmel, X. Gu, R. Trebino, "Highly simplified device for ultrashort-pulse measurement," Opt. Lett. **26**, 932 (2001).
17. A. Christian Silva, "GRENOUILLE - Practical Issues", unpublished.
18. P. O'Shea, M. Kimmel, X. Gu, R. Trebino, "Increased-bandwidth in ultrashort-pulse measurement using an angle-dithered nonlinear-optical crystal," Opt. Express **7**, 342 (2000), http://www.opticsexpress.org/abstract.cfm?URI=OPEX-7-10-342.
19. P. O'Shea, M. Kimmel, R. Trebino, "Increased phase-matching bandwidth in simple ultrashort-laser-pulse measurements," J. Opt. B **4**, 44 (2002).
20. S. Akturk, M. Kimmel, P.O'Shea, R.Trebino, "Measuring pulse-front tilt in ultrashort pulses using GRENOUILLE," Opt. Express. **11**, 491 (2003), http://www.opticsexpress.org/abstract.cfm?URI=OPEX-11-5-491.

1. Introduction

Frequency resolved optical gating (FROG) [1] has been used as a measurement technique in the field of nonlinear fiber optics [2] by several groups. In the regime of wavelengths covered by the mode-locked Ti:Sapphire laser ($\sim$ 810 nm, which lies in the normal dispersion regime of fused silica), such measurements have been carried out notably by Dudley, *et al*. [3] for analyzing the broadband continuum generated by femtosecond pulse propagation through a photonic crystal fiber. Dudley *et al*. [3] also present results of numerical simulations showing agreement with experiments. In the present work, we discuss experimental and computational results for a polarization maintaining fiber made of fused silica. The advantages are that the refractive index of fused silica is well characterized, making it easier to model the experiments with a pseudospectral nonlinear Schrödinger equation based approach [2]. Moreover, a polarization maintaining fiber was used to avoid the random polarization fluctuations that would result if a standard fiber (non-polarization maintaining) were to be used. This made the study of both self-phase modulation (SPM) and cross-phase modulation (XPM) between orthogonal polarizations possible.

Degenerate cross-phase modulation (DXPM) in optical fibers has been studied extensively in the past [4, 5, 6] where asymmetric spectral broadening has been reported and well explained. The works of Nishizawa *et al*. involve the study of cross-phase modulation in optical fibers using FROG. The effects of input pulse asymmetry have not been studied by either of the groups mentioned above. More recently, other groups have studied the evolution of femtosecond pulse

#3084 - $15.00 US Received Septebmer 25, 2003; Revised October 31, 2003
(C) 2003 OSA

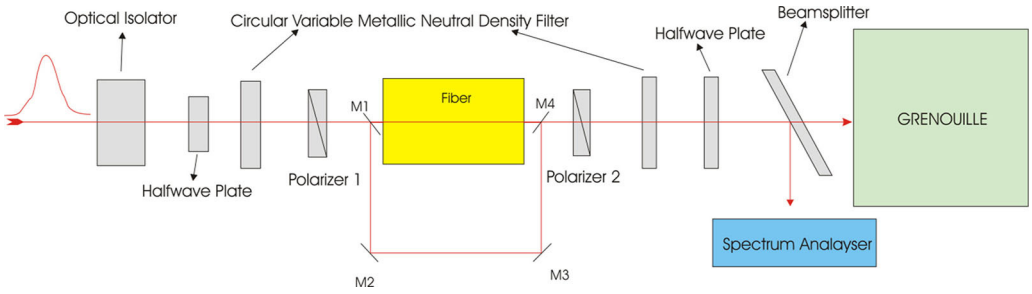

Fig. 1. Block diagram of the experimental setup (not drawn to scale). The optical isolator prevents feedback into the mode-locked Ti:Sapphire laser from the input end of the fiber. The mirrors M1, M2, M3, M4 are placed only when measuring the FROG traces of the pulses input to the fiber. The input half-wave plate, polarizer 1 and polarizer 2 are used such that three possible configurations are studied - $\theta_{in} = \theta_{out} = \pm 45^o, 0^0$, where θ is the angle between the polarization of the input(output) light and the slow axis of the optical fiber. The output half-wave plate is used to rotate the axis of polarization of the output light to match with the axis of the nonlinear crystal in the GRENOUILLE setup. The optical spectrum analyzer is present as a cross-check for the FROG recovered pulses.

propagation through fused silica fibers using FROG in the 1.3 μm and the 1.55 μm regime, notable among them being the works of Omenetto *et al*. [7, 8, 9], Nishizawa *et al*. [10, 11, 12, 13] and Ogawa *et al*. [14]. In particular, the effects of input pulse asymmetry have not been studied by either of the groups.

In the present study, this asymmetry is seen to be the dominant cause of transfer of pulse energy towards longer wavelengths within the pulse (an effect usually attributed to intrapulse Raman scattering [2]). While the studies of Dudley *et al*. and Nishizawa *et al*. rely on cross-correlation FROG (or XFROG [1]), the study of Ogawa *et al*. relies on two photon absorption FROG (or TPA FROG), and the study of Omenetto *et al*. relies on a single-shot SHG-FROG. The apparatus used in the present case is a simplified version of a single-shot SHG-FROG nicknamed GRENOUILLE (Grating Eliminated No-Nonsense Observation of Incident Laser Light E-fields) by its inventors, O'Shea *et al*. [16]. Further, the results are presented in the form of a linear juxtaposition of the spectrogram (or short-time spectral history) [15] of the pulse with its optical spectrum, and its optical time-trace (similar to the nonlinear juxtaposition presented by Dudley *et al*. [3]).

Section 2 discusses the experimental setup used and the method by which the experiment was carried out. Section 3 discusses the numerical model and the results of the simulations that were carried out and compares the results with the experiment. Section 4 provides the conclusion.

2. Experimental setup

Figure 1 shows the experimental setup that is used. The experiments are done with polarized femtosecond pulses from a mode locked Ti:Sapphire laser (Spectra-Physics Tsunami) operating at a central wavelength of $\sim$ 810 nm with a temporal pulse width of $\sim$ 138 fs and a pulse repetition rate of 82 MHz. The laser light is coupled into a short ($\sim$6.9 cm) polarization maintaining optical fiber (Corning PM630, with a cutoff wavelength of 630 nm, a core diameter of $\sim$ 4 μm and a maximum beat-length of 2 mm).

A Photon Inc. Beam Scan at the output end of the fiber is used to ensure that the coupled light has a single-transverse-mode. In order to achieve good coupling ($\sim$70%) without destroying the mode-locked condition of the Tsunami (which is unstable to feedback arising from

#3084 - $15.00 US
Received Septebmer 25, 2003; Revised October 31, 2003
(C) 2003 OSA

reflection, primarily at the input end of the fiber), an optical isolator is placed immediately after the laser. The input power into the fiber is controlled using a metallic variable neutral density filter (VNDF). The combination of a half-wave-plate and a Glan Thompson linear polarizer is used to rotate the polarization of the pulses with respect to the fast and slow axes of the fiber.

Angles of input polarization of 0°, and $\pm 45^\circ$ with respect to the fast(slow) axes are used. In the first case (0°), we propagate pulses along one of the axes of the fiber. This case was chosen as it is easily amenable to modeling by a single nonlinear Schrödinger equation (generalized suitably to include the effects arising due to sub-picosecond pulse width). In the second case, ($\pm 45^\circ$), the light intensity is equally split along the two axes of the fiber. This is done in order to study the phenomenon of self-phase modulation (SPM) and degenerate-cross-phase modulation (DXPM) simultaneously for femtosecond pulses. In this case, interpulse walkoff between pulses traveling along the slow and the fast axes has to be taken into account when the simulations are performed, thus requiring a coupled set of two generalized nonlinear Schrödinger equations (one for each polarization).

Measurements of the full electric field (intensity and phase) of the output pulses are performed using GRENOUILLE [16]. The GRENOUILLE-FROG setup used in our experiments is very similar to that developed by O'Shea *et al*. [16], with the difference being that we use a spherico-cylindrical lens system in front of the CCD camera instead of a bi-cylindrical lens system used in [16].

The optical spectrum of the output pulses is also measured independently using an IST-REES E200 Series optical spectrum analyzer. This is done after the collimated fiber output beam is sent through a Glan Thompson polarizer (Polarizer 2 in Fig. 1), a neutral density filter, a half-wave plate and a beam splitter. The spectrum analyzer is used as a cross-check for the quality of the FROG recovered spectrum. Close agreement between the spectrum recovered using FROG and the one directly measured using the spectrum analyzer is found for the results presented here.

The axis of the output polarizer is chosen parallel to that of the input polarizer for all the three cases investigated (i.e. 0° and $\pm 45^\circ$). For the $\pm 45^\circ$ case, the function of the output polarizer is to generate linearly polarized light by combining (interfering) the light that had propagated along both axes. For pulses traveling along one of the axis of the fiber (0° case), the output polarizer would not be needed (in an ideal situation), since the pulses are linearly polarized upon exiting the fiber. We find it necessary to keep the output polarizer in the experiment in order to retain the beam alignment for the GRENOUILLE and the Optical Spectrum Analyzer diagnostics while changing from the 0° to the $\pm 45^\circ$ cases.

The half-wave-plate after the fiber is needed in order to rotate the polarization of the light after the output polarizer until it is parallel to the axis of the nonlinear SHG crystal used in the GRENOUILLE apparatus. A 512 X 480 Pulnix TM CCD camera is used to photograph the SHG-FROG traces produced by the GRENOUILLE apparatus. A variable neutral density filter is used after the output half-wave-plate in order to prevent saturation of the CCD camera. The FROG traces are recorded on a Dell Dimension desktop PC using a frame grabber. The FEMTOSOFT FROG-retrieval software is used to retrieve the electric field of the pulses from the experimentally measured SHG-FROG traces.

We conducted experiments with power levels ranging from 50 mW to 300 mW of average (cw) power coupled into the optical fiber. The full electric field is recovered for all power levels and for all the three combinations of input and output polarization angles considered. Similar qualitative agreement with simulations are found for all power levels.

In this work, we present results corresponding to a cw power of 140 mW ($\sim$ 40 kW peak power, $\sim$ 6 nJ pulse energy) coupled into the fiber. The resolution of the SHG-FROG is 4.38 fs/pixel and 238 GHz/pixel respectively. The mirrors M1, M2, M3, M4 are placed only when

#3084 - $15.00 US Received Septebmer 25, 2003; Revised October 31, 2003
(C) 2003 OSA

measuring the FROG trace of the pulse input to the fiber. Care is taken to use metallic mirrors only, so that the polarization orientation of the pulses is not modified by the mirrors.

GRENOUILLE can accurately measure a pulse presenting time-bandwidth product (TBP) of up to 10 [16, 17]. The input pulse satisfies these requirements quite well. However, the pulses output from the fiber have a pulse width of $\sim$ 1ps and a bandwidth of $\sim$ 40 THz implying a TBP of 40. Hence the comparisons between experiment and simulation are only qualitatively correct, as we stretched GRENOUILLE to 4 times its maximum capability in terms of TBP.

GRENOUILLE was calibrated using 189 fs, 5.1 nm pulses with 0 chirp (TBP $\sim$ 1), converted into double pulses by passage through an etalon [17, 1]. Similar pulses were also used to accurately measure the beat-length of the fiber by recording the wavelength separation of the modulations produced after passage through 1 m of fiber. However, for our experiments we choose to work with an asymmetric (TBP $>$ 1) pulse configuration of 138 fs and 12 nm bandwidth. In the next section it will be shown that this input pulse asymmetry is instrumental in explaining the nature of the output spectra, which are found to have a transfer of pulse energy towards longer wavelengths.

3. Generalized CNLSE model and comparison with experiments

All the simulations are done with the generalized NLSE using the split step Fourier method (SSFM) [2]. For the off-axis ($\theta = \pm 45^{\circ}$) simulations we are required to simulate two coupled equations, one for each polarization component of the propagating Electric field [2].

$$\frac{\partial A}{\partial Z} = i\gamma P_0 \left(|A|^2 A + \frac{2}{3}|B|^2 A - \frac{T_R}{T_0} A \frac{\partial |A|^2}{\partial \tau} \right) - \frac{i\beta^{(2)}}{2T_0^2}\frac{\partial^2 A}{\partial \tau^2} + \frac{\beta^{(3)}}{6T_0^3}\frac{\partial^3 A}{\partial \tau^3} - \frac{\alpha A}{2} \tag{1}$$

$$\frac{\partial B}{\partial Z} = i\gamma P_0 \left(|B|^2 B + \frac{2}{3}|A|^2 B - \frac{T_R}{T_0} B \frac{\partial |B|^2}{\partial \tau} \right) - \frac{d}{T_0}\frac{\partial B}{\partial \tau} - \frac{i\beta^{(2)}}{2T_0^2}\frac{\partial^2 B}{\partial \tau^2} + \frac{\beta^{(3)}}{6T_0^3}\frac{\partial^3 B}{\partial \tau^3} - \frac{\alpha B}{2} \tag{2}$$

A,B represent the normalized complex electric field envelopes of the two orthogonally polarized pulses traveling through the fiber along the fast axis and the slow axis respectively. Z is the distance along the fiber in meters, τ is the normalized time measured in a frame of reference moving at the group velocity of the pulse along the slow axis [$\tau = (t - Z/v_{gs})/T_0$], where T_0 is the time-scale chosen for the simulations and is of the order of the pulse width ($\sim$ 138 fs FWHM). $\beta^{(2)}$ = 35 ps^2/km is the group velocity dispersion coefficient, $\beta^{(3)}$ = 0.1 ps^3/km is the third order dispersion coefficient, $\alpha \sim$6 dB/km = 0.0014 m^{-1} is the optical loss in the fiber material, and γ = 0.019 /Wm is the nonlinearity coefficient of the fiber for the central wavelength of 810 nm of the pulses [2]. P_0=40kW is the peak power of the input pulses corresponding to a cw power of 140 mW and a pulse energy of 5.5 nJ. d $\sim$ 2.2 ps/m is the polarization mode dispersion coefficient or pulse walk-off parameter which governs the rate of walk-off between the two orthogonally polarized pulses propagating along the two axes of the fiber and can be calculated from the experimentally estimated beat-length. T_R ($\sim$ 3 fs) [2] represents the slope of the Raman-gain function for the operating frequency.

The following length scales give an idea of the processes involved and their relative importance in the dynamical evolution of the pulse along the fiber length :

$$L_{NL} = \frac{1}{\gamma P_0} \sim 1.3mm$$
$$L_w = \frac{T_0}{d} \sim 6.3cm$$

#3084 - $15.00 US Received Septebmer 25, 2003; Revised October 31, 2003
(C) 2003 OSA

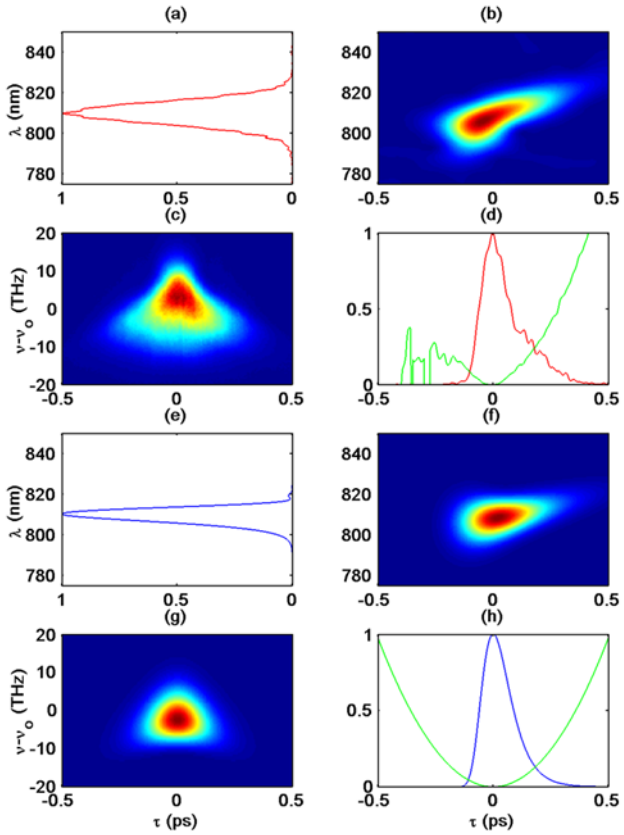

Fig. 2. Coupled into the fiber FROG traces: measured (c) and assumed in the simulation (g). Measured, from the FROG algorithm recovered spectrum (a) and time trace (d). Used in the simulation spectrum (e) and time trace (h). Spectrograms: measured (b) and used for the simulation (f).

$$L_{D_2} = \frac{T_0^2}{\beta^{(2)}} \sim 54cm$$
$$L_{D_3} = \frac{T_0^3}{\beta^{(3)}} \sim 26m$$
$$L_{IRS} = \frac{T_0}{T_R} L_{NL} \sim 6cm$$
$$L_\alpha = \frac{1}{\alpha} \sim 700m \quad (3)$$

”NL” stands for nonlinear, ”w” for linear pulse walk-off arising due the difference in group velocities between the slow and the fast axes, ”D_2” and ”D_3” stand for 2nd and 3rd order dispersion respectively, ”IRS” stands for intrapulse Raman scattering, and ”α” stands for fiber loss [2].

The nonlinear length is the smallest, indicating that nonlinearity played a dominant role. The linear walk-off length is comparable to the fiber length indicating that its effect is considerably

#3084 - $15.00 US Received Septebmer 25, 2003; Revised October 31, 2003
(C) 2003 OSA

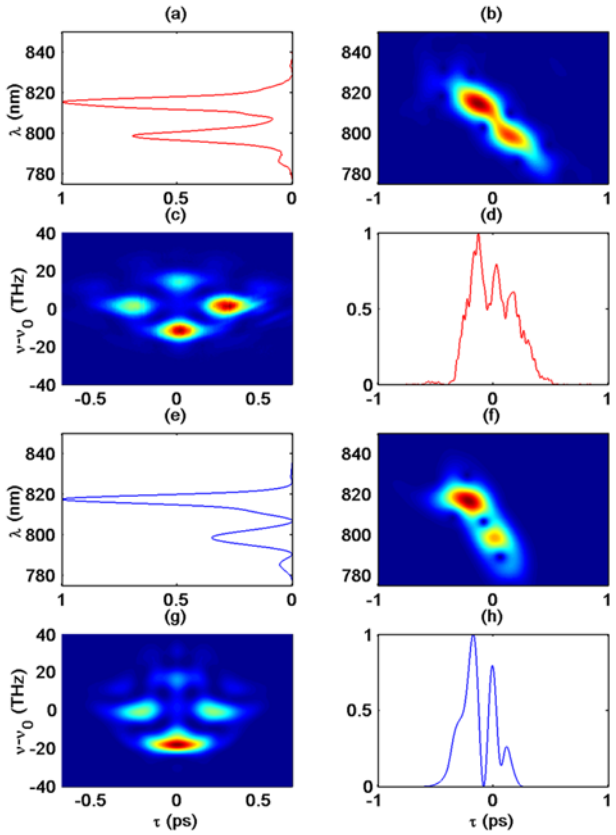

Fig. 3. Experimental (a to d) and Simulated (e to h) figures for $\theta = -45^{\circ}$. t-λ spectrograms (b & f) for $\theta = -45^{\circ}$ juxtaposed with corresponding time-trace (d & h), optical spectrum (a & e) and SHG-FROG trace (c & g).

less important. Since we are interfering pulses that are propagating along both axis of the fiber, this small effect is greatly increased giving the maximum interference at the 45° angle. L_{IRS} is of the order of the fiber length and the above comparison of length scales indicates that IRS should be of little importance in the dynamics. This is observed to be the case with the numerical results. All the asymmetry in the output pulse, which is generally attributed to IRS, is found to be primarily due to the asymmetry of the input pulse. The asymmetry of the input pulse plays an important role in its spectral evolution. The input pulse has a leading edge, as seen in Fig. 2(d), and causes (as a result of the simulations) a transfer of pulse energy towards longer wavelengths. This is an effect similar to the self-frequency shift caused by IRS. Simulations carried out ignoring IRS but including pulse asymmetry give the same results as the simulations including both IRS and pulse asymmetry. Conversely, simulations carried out including IRS but ignoring pulse asymmetry give too weak a transfer of pulse energy towards longer wavelengths compared to the experiments. The modulation lobes visible in the simulated optical spectra for the $\pm 45^{o}$ cases are very weak or even absent in this case. For these reasons, we conclude that IRS did not play an important role in the dynamics, although it is likely to gain importance for longer fiber.

#3084 - $15.00 US
Received Septebmer 25, 2003; Revised October 31, 2003
(C) 2003 OSA

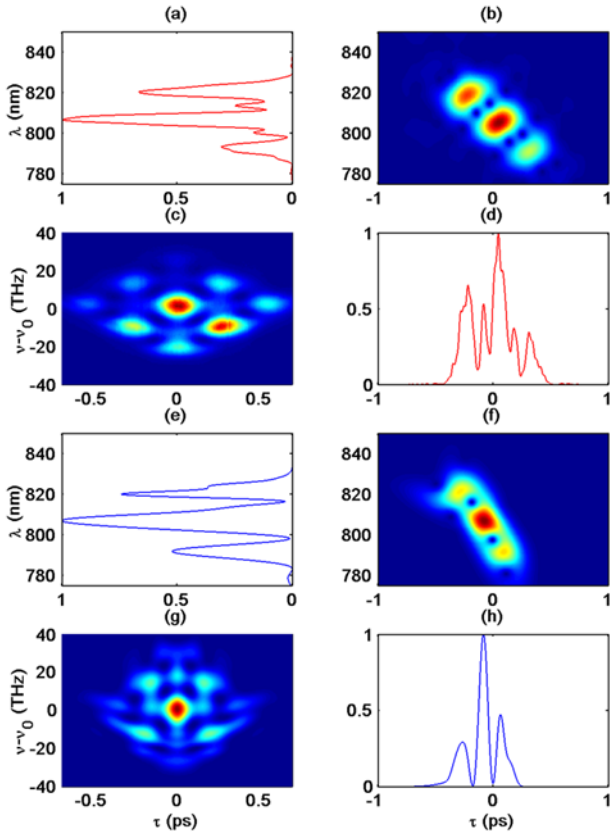

Fig. 4. Experimental (a to d) and Simulated (e to h) figures for $\theta = +45^{\circ}$. t-λ spectrograms (b & f) for $\theta = +45^{\circ}$ juxtaposed with corresponding time-trace (d & h), optical spectrum (a & e) and SHG-FROG trace (c & g).

The equations are integrated using the split-step Fourier method (SSFM) [2], a step size ΔZ = 0.1 mm is found to be sufficiently small for convergent results. The method assumes the slowly varying envelope approximation which is a good approximation in the present case.

The SHG-FROG trace for the pulses is defined as [1]

$$I_{FROG}(\omega,\tau) = |\int_{-\infty}^{+\infty} dt E(t)E(t-\tau)e^{i\omega\tau}|^2 \tag{4}$$

and is a special form of the spectrogram or short-time spectral history [15]

$$S(\omega,\tau) = |\int_{-\infty}^{+\infty} dt E(t)g(t-\tau)e^{-i\omega\tau}|^2, \tag{5}$$

where g(t-τ) is a variable-delay gate function [1]. g(t-τ) = E(t-τ) is a natural choice of the gate function for the experiment (i.e., gating the Electric field of the pulse with itself, since only the optical pulse itself, has a time-scale small enough to be comparable to its own femtosecond time-scale) [1]. The time-trace and the optical spectrum of the input and output pulses can be computed from the SHG-FROG trace using the FEMTOSOFT FROG algorithm software. The

#3084 - $15.00 US
Received Septebmer 25, 2003; Revised October 31, 2003
(C) 2003 OSA

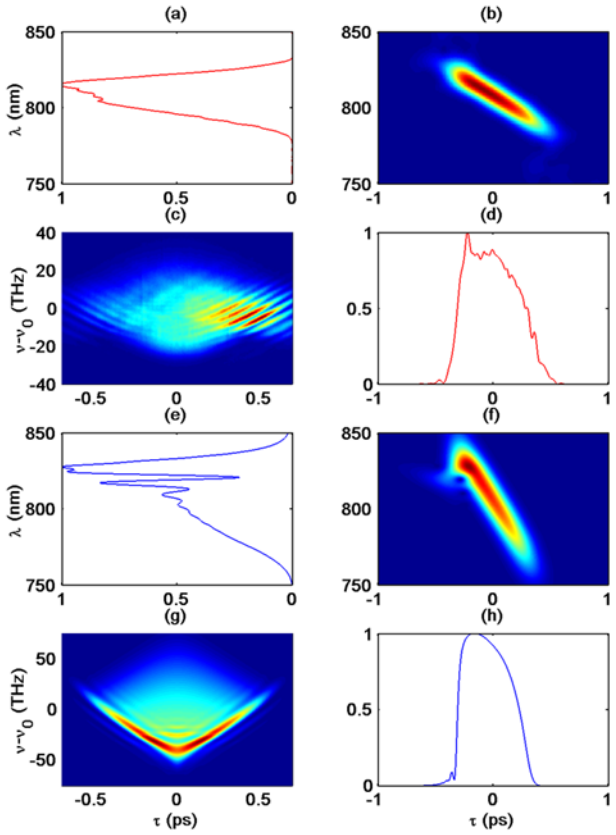

Fig. 5. Experimental (a to d) and Simulated (e to h) figures for $\theta = 0^o$. t-λ spectrograms (b & f) for $\theta = 0^o$ juxtaposed with corresponding time-trace (d & h), optical spectrum (a & e) and SHG-FROG trace (c & g).

SHG-FROG representation, however, is not the most intuitive for comparison with the recovered time-trace and spectrum. No linear, one-to-one correspondence is seen between features in the SHG-FROG trace and features in the time-trace and optical spectra upon juxtaposition. Moreover, it is difficult to discern the temporal evolution of the spectral content of the pulse from its leading edge to its trailing edge by looking at the SHG-FROG trace. In this sense, the SHG-FROG trace is not the most intuitive representation of the time-wavelength structure of the pulse. A time-wavelength spectrogram or short-time spectral history is computed from the recovered Electric field time-trace using the gate function given below

$$g(t-\tau) = exp - \frac{(t-\tau-t_{win})^2}{2}. \tag{6}$$

t_{win} is the size of the window-width chosen for the Gaussian gate. It is important to choose t_{win} to be smaller than the temporal extent of the output pulses. However, care must be taken to keep t_{win} large enough to have a good wavelength resolution in the spectrogram. The value chosen in the present case is t_{win} = 0.2 ps (FWHM) which is smaller than the temporal extent of the output pulses ($\sim$ 1.5 ps) but larger than the input pulse (0.138 ps FWHM). This is an invertible representation [15] and the SHG-FROG trace can be recovered from it with knowledge of the

#3084 - $15.00 US
Received Septebmer 25, 2003; Revised October 31, 2003
(C) 2003 OSA

gate function.

Figure 2 shows experimental and simulated versions of the input pulse, its time-trace, spectrogram, optical spectrum and FROG trace juxtaposed in such a way that it is visually possible to correlate corresponding features such as peaks and troughs between the spectrogram, the optical spectrum and the time-trace. Such a juxtaposition is not possible with the SHG-FROG traces. Such a juxtaposition is also presented by Dudley *et al*. [3] with an XFROG trace serving as a spectrogram. The deficiency of their juxtaposition is that the wavelength scale of the optical spectrum has to be stretched nonlinearly for an accurate comparison. Figure 2(c) represents the measured SHG-FROG trace. Figures 2(a) and 2(d) represent the input optical spectrum and optical time-trace recovered from the FROG trace shown in Fig. 2(c) using the FEMTOSOFT FROG software. Figure 2(b) represents the experimental input spectrogram computed from the FROG trace in Fig. 2(c). Figures 2(e)-2(h) represent the corresponding input pulse characteristics of the assumed input pulse for the simulations. The green curve in both Figs. 2(d) and 2(h) represents the phase of the input electric field with time. Note the asymmetry in the experimentally measured input time-trace (2(d), intensity (red-curve)), which is reproduced to a certain extent in the input pulse used for the simulations (2(h), intensity (blue-curve)). The input pulse is assumed to be linearly chirped (hence the parabolic phase distribution (green curve in Fig. 2(h))).

Figures 3,4 and 5 give similar juxtapositions for the output pulses, for the θ=-45°, +45° and 0°, respectively. In all three cases a clear shift of pulse energy towards longer wavelengths can be seen. This is attributable to the effects of SPM and DXPM with the effects of SPM being stronger(due to the 2/3 factor in Eqs. 1 and 2). Moreover, the strong asymmetrical spectral broadening observed, can be easily explained by self-phase modulation effects. If the initial optical pulse presents a strong temporal asymmetry with a steep leading edge, SPM will generate more Stokes frequencies than anti-Stokes frequencies, thus resulting in an overall red-shift. In Figs. 3 and 4 the temporal and spectral modulations seen arise from interference between the two output polarization components of the pulse that are coherently combined by the output polarizer. These modulations are due to pulse walk-off or polarization mode dispersion.

The simulations are found to be very sensitive to the exact nature of the input pulse. That is, the intensity and phase of the numerically assumed input pulse has to be as close as possible to that of the actual input pulse coupled into the fiber in the experiments. The experimentally measured input trace used in this work is shown in Fig. 2 along with its corresponding optical spectrogram juxtaposed with the recovered time-trace and optical-spectrum. The input pulse assumed for the simulations is a pulse analytically fitted to the experimental input pulse with the following asymmetric analytic function:

$$U_x(t,0) = \exp\left[1+\tau-\exp(-\tau)+ic\tau^2\right] \tag{7}$$

which can also be expressed as

$$U_x(t,0) = \exp\left[-\frac{\tau^2}{2}\left(1-ic-\frac{\tau}{3}+\frac{\tau^2}{12}-\frac{\tau^3}{60}+...\right)\right], \tag{8}$$

where $\tau = t/T_0$, $T_0 \sim$ 86 fs and c $\sim$ -0.32 are the 2 parameters used in defining the analytic function. The values of these 2 parameters are found by using the nonlinear least square fitting.

In all the output experimental FROG traces, i.e., Figs. 3(c), 4(c), and 5(c), the mirror reflection symmetry characteristic of SHG-FROG traces is seen to be absent. This is possibly due to pulse-front tilt [20]. This is partially taken into account by the FEMTOSOFT FROG algorithm which "knows" that the traces are SHG-FROG traces [1]. Since the results are qualitative, this is a minor discrepancy. Looking at the $\pm$45° cases, it is observed that both the experimental and simulated spectrograms have the same number of lobes. This feature is also seen in the

#3084 - $15.00 US Received Septebmer 25, 2003; Revised October 31, 2003
(C) 2003 OSA

optical spectra and to a certain extent in the optical time trace, too. The bandwidths and pulse widths of the simulated and experimental pulses are observed to be similar. The spectrogram representation is well suited for simultaneous comparison with both the optical spectrum and the optical time-trace (red curves - experimental, blue curves - simulation). The optical spectrum and the optical time-trace can be viewed as orthographic projections of the spectrogram. Good qualitative agreement is seen between simulations and experiment.

4. Conclusion

We have measured and characterized nonlinear modulations (SPM and DXPM) of asymmetric femtosecond pulses propagating through a short birefringent single mode fiber both experimentally and numerically. We observe good qualitative agreement between GRENOUILLE based experiments and CNLSE based simulations. We present the results using a linear spectrogram (short time spectral history) function of a pulse which is then juxtaposed with its optical spectrum and time-trace for easy visual comparison. It is observed that the output pulses are highly asymmetric towards longer wavelengths; this asymmetry is determined to be caused by asymmetry in the input pulse's temporal profile and not by IRS governed self-frequency shift. We have measured pulses having a TBP of 40, well over the advisable limit of 10 [16] for GRENOUILLE. Recent improvements in the maximum measurable bandwidth of GRENOUILLE [18, 19] may help in making the present and similar results more quantitative. The results of this investigation indicate that a possible practical application would be to modulate short pulses, both temporally and spectrally, by passage through such polarization maintaining optical fibers with specified orientation and length.

Acknowledgments

We gratefully acknowledge help from Patrick O'Shea, Mark Kimmel and Rick Trebino of the FROG team at Georgia Tech in setting up the GRENOUILLE, from Ryan McAllister and from Donald Martin for general technical support. This work was supported by the Office of Naval Research, Physics Division.

#3084 - $15.00 US Received Septebmer 25, 2003; Revised October 31, 2003
(C) 2003 OSA